Raman identification of pigments and opacifiers: Interest and limitation of multivariate analysis by comparison with solid state spectroscopical approach-II. Arsenic-based opacifiers and relation with cobalt ores

Jacques Burlot, Divine Vangu, Ludovic Bellot-Gurlet, Philippe Colomban

Received: 28 July 2023 | Revised: 22 September 2023 | Accepted: 2 October 2023

DOI: 10.1002/jrs.6612

SPECIAL ISSUE - RESEARCH ARTICLE

Journal of RAMAN SPECTROSCOPY WILEY

Raman identification of pigments and opacifiers: Interest and limitation of multivariate analysis by comparison with solid state spectroscopical approach—II. Arsenic-based opacifiers and relation with cobalt ores

Jacques Burlot | **Divine Vangu** | **Ludovic Bellot-Gurlet** | **Philippe Colomban**

CNRS, de la Molécule aux Nano-objets: Réactivité, Interactions et, Spectroscopies, MONARIS UMR8233, Sorbonne Université, Paris, France

Correspondence
Philippe Colomban, Sorbonne Université, CNRS, de la Molécule aux Nano-objets: Réactivité, Interactions et, Spectroscopies, MONARIS UMR8233, 4 Place Jussieu, 75005 Paris, France.
Email: philippe.colomban@sorbonne-universite.fr

Funding information
Agence Nationale de la Recherche, Grant/Award Number: 19-CE27-0019-02

Abstract

Raman analysis is a noninvasive technique that can be conducted on-site via a mobile system. However, the presence in variable quantity of different crystalline or amorphous phases (glassy matrix, opacifiers and pigments) in the enamel leads to the partial observation of Raman signatures, signatures often not being characterized in the literature. We study here the phases observed in the white, blue and yellow/green enamels of French and Chinese objects from the 18th century and compare the effectiveness of a solid-state spectroscopic approach (identification of the parameters determining the vibrational modes in relation to the structures) and the multivariate chemometric approach (PCA and Hierarchical Clustering), carried out on the global or partial spectra, or on the parameters extracted from the first approach. The incorporation of the spectra of neighbouring or similar phases from the literature into the corpus of processed data, in particular those obtained for phases that are not initially structurally characterized, is decisive for the quality of the results. At least four different lead arsenates are identified. The combination of visual observation of the peaks and multivariate analysis shows that the shape, position and area of the band associated with the main As-O stretching vibration around 820 cm^{-1} vary according to several criteria related to production techniques specific to certain workshops. The contribution of multivariate analysis based on spectra alone appears to be very limited compared to the examination of spectroscopic parameters.

KEYWORDS

arsenic, blue, cobalt, enamels, PCA

1 | INTRODUCTION

Raman analysis is a noninvasive technique which can be conducted on-site with a mobile set-up, which is particularly interesting for studying outstanding ancient objects whose transport and insurance costs are too high for them to be studied in the laboratory.[1–4] The limited availability of objects means that it is not always possible to run several analysis campaigns with different analytical instruments. As a result, in our case, which concerns the study of enamelled objects, the identification of the agents constituting the decoration—generally the most sophisticated and informative part in terms of the history of ceramic art and techniques—has to be based on Raman spectroscopy alone or in association with elemental composition of the "surface layer" measured with pXRF. The sophistication of painted enamelled decors means that the coloured layers are composite materials composed firstly of a glassy silicate matrix. This is a complex silicate whose processing parameters (melting temperature, viscosity, thermal expansion mismatch with the substrate) are adjusted by the incorporation of fluxes (based on alkaline and alkaline-earth, lead and boron oxides). Crystalline phases—residues of the initial raw materials (quartz, feldspar, anatase, rutile, etc.) or modified/formed during the firing process(es) (cristobalite, tridymite, feldspar, rutile, etc.)—as well as pigments and opacifiers deliberately introduced or formed during the thermal cycle by nucleation-precipitation[5] are embedded in the glassy silicate matrix.

While the use of very high magnification optics (×50, ×100 or even ×200) enables us to probe volumes ranging from tens μm^3 to less than 1 μm^3 in air, that is, close to the pigment grain size, the dispersion of the laser focusing spot in the solid phase and the very large differences in Raman cross-section between phases mean that it is very rare to obtain a "pure" spectrum corresponding to a single phase.[6] In addition, the great diversity of pigments in terms of structure and composition (most phases made from natural raw materials are nonstoichiometric) means that reference spectra in the literature, when they exist for the structure in question, rarely correspond to phases with the specific compositions/structures found in glazes pigments or opacifiers. Moreover, for many coloured phases, laser–matter interaction leads to resonance phenomena that strongly affect the component of the Raman spectra as a function of the exciting laser wavelength and reference data should have been recorded using same conditions.

We are evaluating here different approaches to Raman signature analysis: the multivariate analysis approach (PCA and Hierarchical Clustering) on the whole or reduced parts of the spectrum, the reasoned solid-state spectrochemical analysis on spectroscopic parameters extracted from the fitted spectra and the combination of these two approaches.[7–9] In a companion paper[10] in this same special issue, we focused on Pb-Sn-Sb-based pigments (the tin-lead yellow and Naples yellow family). We focused here on lead arsenate opacifiers. This opacification may be voluntary, as in Venetian *lattimo* glass and certain 17th-century glass products,[11] but it may also result from the use of European cobalt ores that are very rich in arsenic,[12,13] which, by providing both cobalt and arsenic, enable beautiful blues to be obtained in oxidizing firing atmosphere, whereas this is not possible using Asian ores that are very rich in iron and manganese.[13] This Fe- and Mn-richness of cobalt ores was not a problem for Chinese blue-and-white porcelain fired in a highly reducing atmosphere,[14,15] as the Fe and Mn ions in reduced form do not colour significantly in the visible range. Since our preliminary works[5,16,17] have shown a high variability in Raman signatures of Pb- and As-based opacifiers, some corresponding perfectly to the apatite phase ($Na_{1-x-y/2}K_xCa_yPb_4(AsO_4)_3$)[5,17] studied by Manoun et al.,[18] and others, showing differences, in this work we will study these signatures on the same corpus as that used for the Naples yellow family.[10] The corpus concerns enamelled objects produced in Europe and China in the 17th and 18th centuries, that is, under the reigns of kings Louis XIV, the Regency, Louis XV and Louis XVI on the French side, and on the other, in China, under the Qing Dynasty (reigns of Kangxi, Yongzheng and Qianlong Emperors). Comparing materials evidences for the use of specific phases in the objects produced for the courts of France and China, Chinese and French historical documents report the importation of ingredients and recipes by the Jesuits present at the Manchu Court.[14] Let us recall that China exported large quantities of enamelled porcelain in the 18th century, but previous works demonstrated that these exported porcelains are also enamelled using recipes or even ingredients imported from Europe.[14,15,19,20]

2 | EXPERIMENTAL

2.1 | Studied artefacts

The Raman data set under consideration here is composed of measurements previously carried out on series of blue, white, but also pink, yellow and green enamels from a corpus of European artefacts consisting of watches with sophisticated enamel decoration on metal produced almost exclusively in France (mid-17th to mid-18th century),[21] and French porcelains, mainly of the soft-paste type (late 17th to mid-18th century).[22,23] They also

include Chinese painted and *cloisonné* enamels on metal objects (18th century, during the reigns of Yongzheng (1722–1735) and Qianlong (1735–1796) of the Qing Dynasty) and on porcelains assumed to have been made for the Emperor, some of which are thought to have been produced in the Forbidden City workshop (Zaobanchu, 造辦處, Beitang, Beijing, named *huafalang* 畫琺瑯 or *falangcai* 琺瑯彩), or in the imperial kiln of Jingdezhen (named *yangcai* 洋彩).[5,17,24] Pieces produced specifically for export in official kilns (*waixiao ci* 外銷瓷) or in private kilns (armorial and "*Chine de Commande*" Export porcelains) are also included.[20] The list of artefacts and some of their characteristics are given in Table S1.

2.2 | Raman spectra and fitting

The Raman spectra considered in this paper have been previously published and discussed.[5,17,21–24] They were recorded using a mobile Raman set-up consisting of an HE 532 spectrometer (Horiba Scientific, Jobin-Yvon), a SuperHead® remote measurement head (Horiba Scientific, Jobin-Yvon) equipped with either a ×50 (NA = 0.55, Nikon) or a ×200 (NA = 0.62, Mitutoyo) long working distance microscope objectives (of 17 and 13 mm respectively), and a frequency-doubled Nd:YAG laser of 300 mW (Ventus Quantum). Optic fibres are used to transmit light signals between the different elements. The laser power, adapted and measured to the sample, ranges between 15 (colourless glaze) and 2 mW (dark coloured enamel).

Spectra selected from the literature[18,25–28] were used as reference. They are presented in Figures 1 and 2. In order to incorporate these spectra from the literature into the corpus of spectra for our studies, they were digitized using the following process. They were first converted from the original PDF of the articles to an image in .jpeg format using Able2Extract® (Investintech.com Inc., version Professional 15.0) and then converted into a digital table using WebPlotDigitizer (version 4.5), software that is available online with free access.[29] This second step involves loading the image of the spectra and then aligning and calibrating the axes corresponding to the Raman wavenumber (expressed in cm^{-1}) and the intensity. By

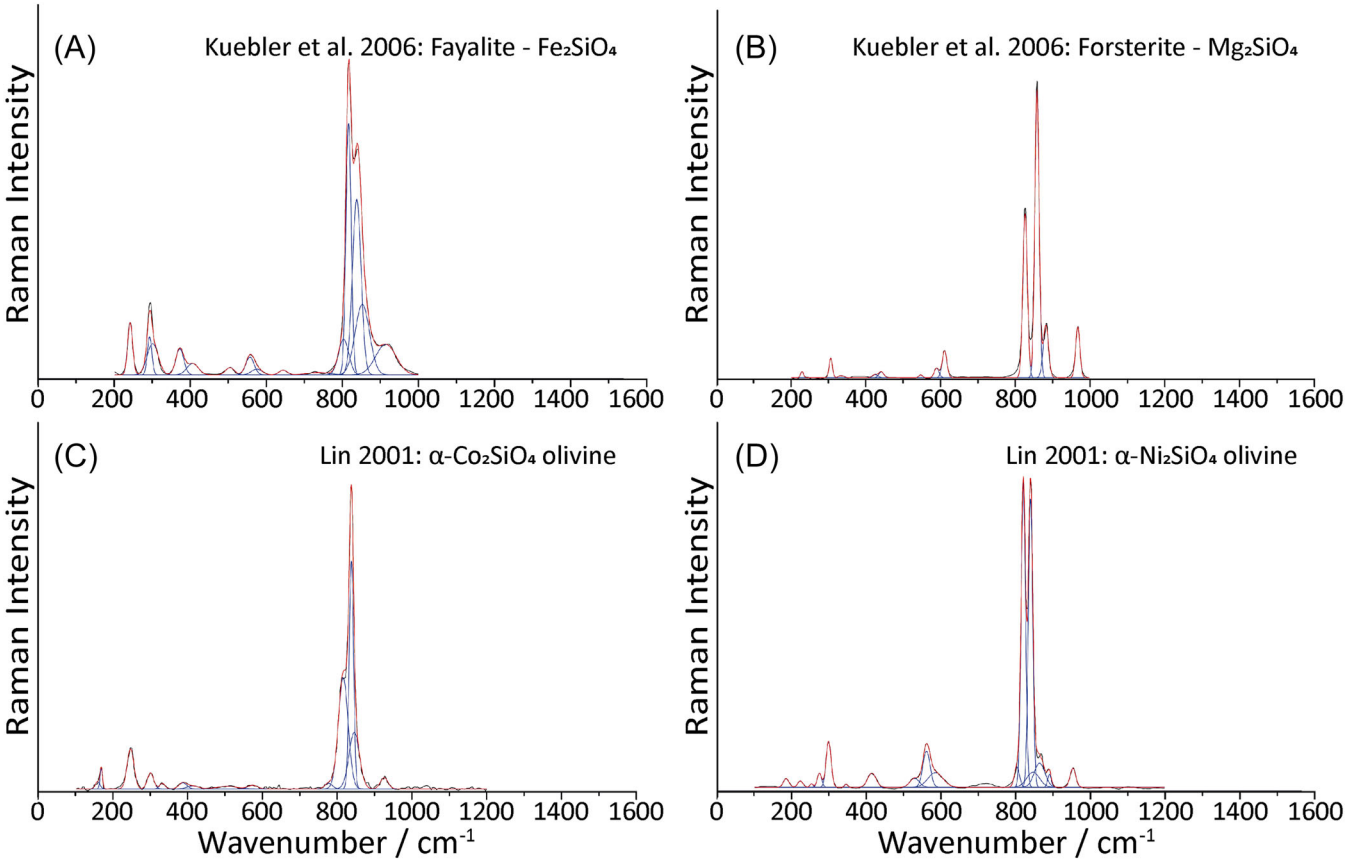

FIGURE 1 Selection of representative spectra from literature (A and B from Kuebler et al.[30] C and D from Lin[31]), corresponding to different olivine compositions, featuring a main Raman peak at ~820 cm^{-1}.

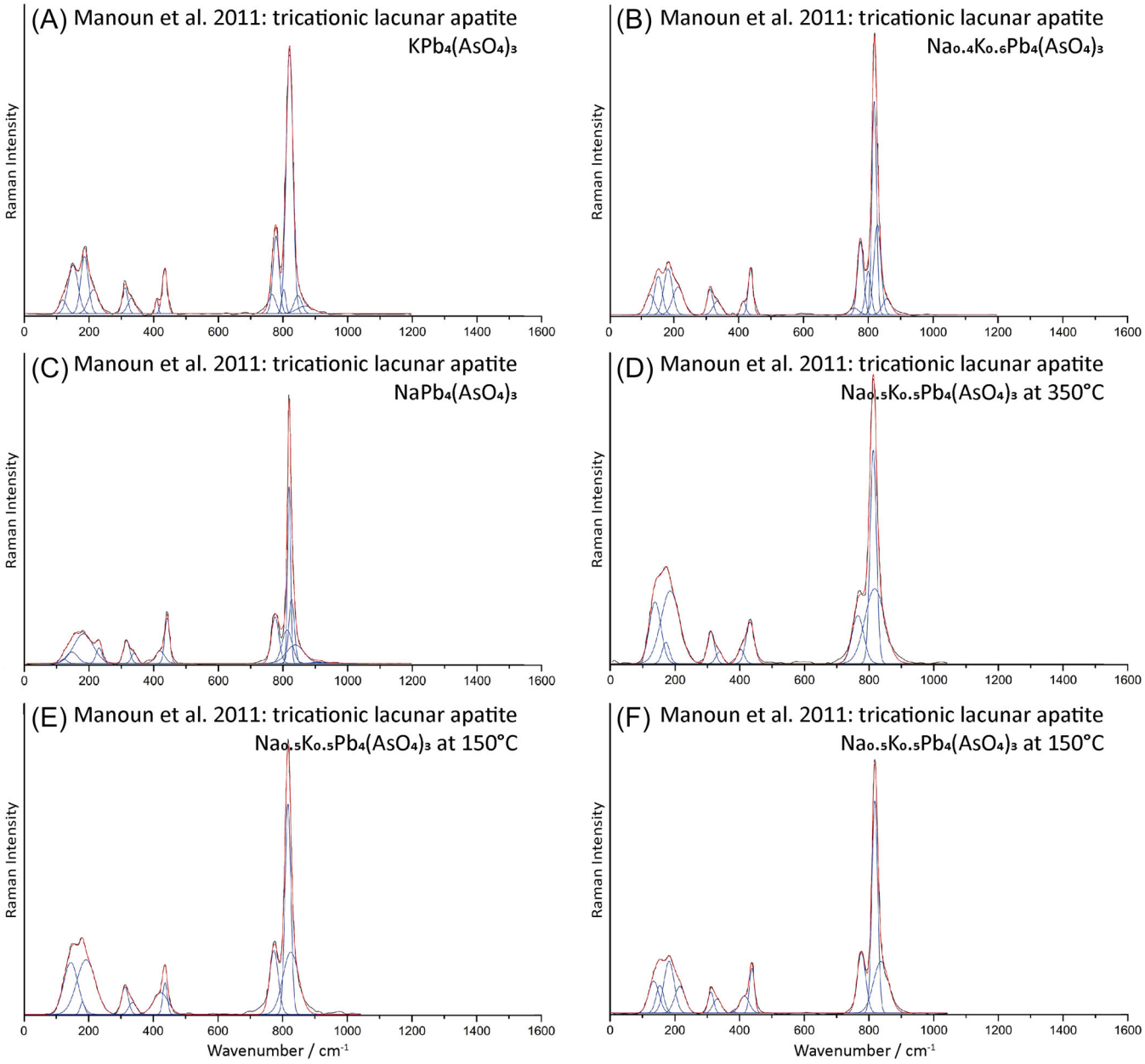

FIGURE 2 Selection of spectra of different apatite phases (A to F) presented in Manoun et al.[18] The different formula is indicated. See reference for details.

selecting the colour corresponding to that of the spectrum on the image, it is then possible to extract the coordinates of the spectrum data points in .csv file format and thus save the spectrum in .txt format usable on standard Raman spectroscopy or data processing software.

Whether for the spectra of our studies or those obtained from the literature,[18,25–28,30,31] a linear segment baseline was subtracted using Labspec® software (5.25.15, 2007, Horiba Jobin-Yvon[6,32]) and the spectra were then decomposed into a sum of elementary bands using Peakfitting Origin® software (6.0, 1999, Microcalc Inc.).

2.3 | Multivariate analysis

After baseline correction (Figure 3A), the spectra were normalized with the online ChemFlow® (version 20.05)[33] software following the Singular Normal Variate (SNV) transformation (Figure 3B), notably to normalise variations in spectral intensities.[34] The SNV transformation, method introduced by Barnes et al.,[35] sees each spectrum having its mean value subtracted and being then divided by its standard deviation, such as its new mean and standard deviation are 0 and 1, respectively. Principal component analyses (PCA) are then performed, again using

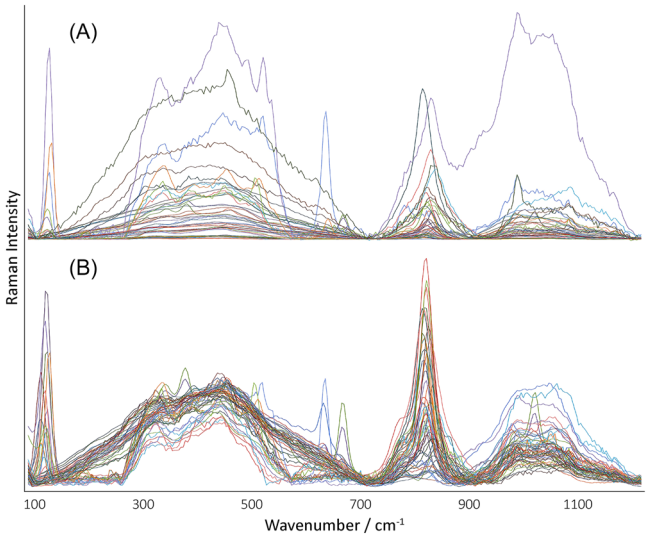

FIGURE 3 Raman spectra of the studied objects ($n = 52$): (A) after baseline subtraction; (B) then after singular normal variate (SNV) transformation.

ChemFlow®, with a calculation based on a maximum of 20 principal components. The first PCA was conducted only within the 730–880 cm^{-1} wavenumber range. Within the same range, a hierarchical clustering (HC) was also performed using the Euclidian distance and the Ward's aggregation rule on the spectra of the studied objects and of the ones from the literature as well. A second PCA was then conducted using as variables the parameters characterizing the elementary bands assigned/related to the As-based compounds (i.e., ~820 cm^{-1} and its shoulder at ~775 cm^{-1}) obtained from the spectral decomposition procedure of our spectra and those from the literature (the values of the width [FWHM], area and centre of gravity of the peaks).

PCA analyses are mainly performed on all samples (those considered as "references" and those studied considered as "unassigned") in order to perform the calculation and examine their groupings. For some PCA diagrams, to facilitate reading, we will first comment on the clustering of references alone, and then on that of enamel samples. In addition, other PCA analyses are performed only on the enamels corpus.

3 | RESULTS

3.1 | Considering the different phases having Raman peak in ~800–850 cm^{-1} range

Before the 1970s, blue colouring of glassy silicates could only be achieved by a few processes, the oldest being the dissolution of Co^{2+} ions in the amorphous lattice of more or less polymerized SiO_4 tetrahedron (no direct vibrational contribution from the presence of cobalt[36] is expected in Raman spectroscopy except the light absorption that flattens the background). Another process involves the dispersion—or nucleation-precipitation—of phases already coloured blue, such as Egyptian blue ($CaCuSi_4O_{10}$)[37,38] or its Han equivalent ($BaCuSi_4O_{10}$),[39,40] lapis lazuli,[41,42] spinels ($CoAl_{2-x}M_xO_4$)[43–45] or cobalt-based olivines ($CoSiO_4$).[30,31] These phases are rather well characterized by Raman signatures outside the range considered for the arsenate-based phases, except for olivine-type structures whose main Raman bands are located around 800–820 cm^{-1}, that is, in the same wavenumber range as the As-O stretching mode (Figure 1). In some cases, these references have been also characterized by elemental analysis.[30]

Contrary to some interpretations that attribute the band observed around 820 cm^{-1} to $CoSiO_4$,[46–48] in association with XRF evidence of Co element, we have pointed out that the strong approximately 820 cm^{-1} band is generally the fingerprint to the formation of arsenate(s) in relation with the use of arsenic-rich cobalt ore (or smalt) of European origin.[14,15] Consequently, we will consider both types of Raman signatures in Figures 1 and 2.

Figure 4 shows the different types of Raman signature that we identified visually in enamelled artefacts, respectively a case (4A) where the signature around 820 cm^{-1} is absent (i.e., a signature corresponding only to that of the glaze, the silicate matrix without crystalline phase), a case (4B) where it is weak, a case (4C) where it is very strong and corresponds exactly to that of the compound $Na_{1-x}K_xPb_4(AsO_4)_3$ of Manoun et al.,[18] and a case (4D) in which the band at 820 cm^{-1} is broadened. The latter band can be explained by a disorder-induced broadening, which could correspond either to a small size of the crystals (nanoparticles), or to a particular disordered structure.

3.2 | Considering the variability of Raman signatures

In Raman scattering, the symmetrical stretching mode is generally the most intense, since it maximizes the deformation of the chemical bond's electron cloud. In the case of most of silicates, for example, olivine, this will be the stretching of the Si-O bond of the SiO_4 tetrahedron. In the case of arsenates, it is the As-O bond of the AsO_4 tetrahedron. Indeed, due to the T_d symmetry of XO_4 tetrahedron and its geometrical stability that prevent distortion, its Raman spectrum is dominated by the A_{1g} symmetric stretching mode and the contribution of the three

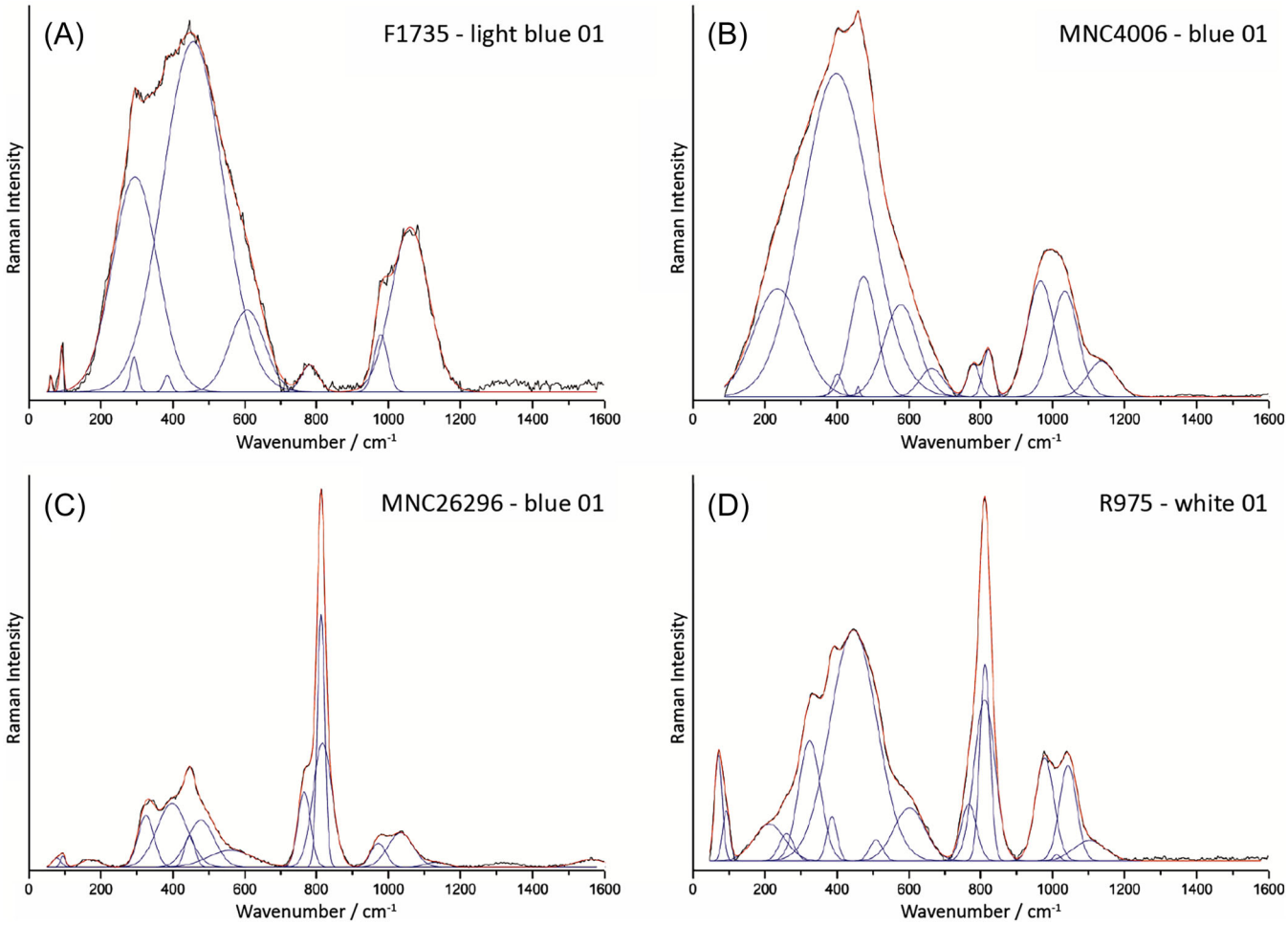

FIGURE 4 Representative spectra of the different Raman signatures profiles obtained for the studied enamels. Spectral decompositions were obtained after subtracting a baseline using a Lorentzian shape for narrow peaks, a Gaussian shape for broad peaks and minimizing the number of bands: (A) no characteristic As–O peak; (B) weak As–O peak (around 820 cm^{-1}); (C) characteristic peak of apatite (775 and 820 cm^{-1} doublet); (D) broad band around 820 cm^{-1} of a disordered phase containing As–O bonds.

antisymmetric modes (F character) can be neglected.[49,50] As the As-O bond involves more electrons, the intensity of the corresponding band is expected to be stronger than that of the Si-O bond.

The distribution of the spectroscopic data extracted by spectral decomposition is presented in Figure 5. Data are classified according to the wavenumber of the band at approximately 820 cm^{-1} and the total area of the band. Five groups can thus be identified on this graph. The three boxed areas B_5 to C'_5 can be considered as characteristic of rather similar phases, since they are distinguished by small shift of the position of the main band of the As-O bond in their respective Raman signatures. The position of the main band for samples in zone A_5 is above 829 cm^{-1}, while it lies between 818 and 823 cm^{-1} for signatures in zone B, and below 816 cm^{-1} for those in zones C_5 and C'_5. The differentiation between the latter two

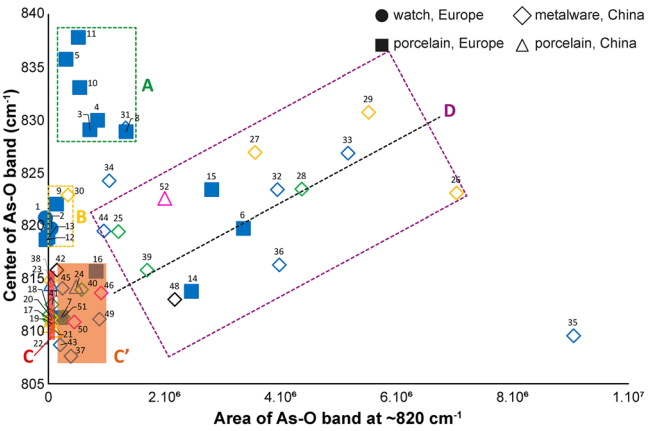

FIGURE 5 Distribution of the values of the Raman wavenumber of the peak of the main As-O bond versus the total area of the band at approximately 820 cm^{-1}. The numbers indicated correspond to the labels of Table S1.

groups is based on the different area of the band at ~820 cm^{-1} which is larger for the C'_5 samples and very narrow for C_5 group. If we have a look at the type of artefacts present in these groups, we can see (Figure 5) that:

i. Group A_5 for which the band position is higher than 829 cm^{-1} contains only French soft-paste porcelains (#3–4: MNC17063; #5: MNC18433; #8: MNC13371; #10: MNC18342; #11: MNC4027, see artefacts in Table S1), as well as a blue enamel of cloisonné decoration of the Chinese metal object F1467C (#31). As the wavenumber range considered could also include signatures corresponding to chromate phase,[14,44] these can be found in this group.
ii. Group B_5 includes the two European enamelled watches (#1: OA10079 and #2: OA8435), as well as three French soft-paste porcelains (#9: MNC4006; #12: MNC8800 and #13: MNC8102) and a yellow cloisonné enamel from Chinese object F1467C (#30).
iii. Group C_5 includes only Chinese objects, as we find three overglaze enamels on the porcelain F1429C (#21–23), and painted and cloisonné enamels on Chinese metal ware (#17–20: F1341C; #38,41: R957).
iv. Group C'_5 represents a greater diversity of objects and decorations—the vast majority of which are nonetheless Chinese—since it includes two French soft-paste porcelains (#7: MNC13371 and #16: MNC25330), but also painted and cloisonné enamels on Chinese metal ware (#37: F1698C; #40,42–43,45–46: R957 and #49–51: R975), as well as one overglaze enamel on Chinese porcelain (#24: F1429C). For this group, which corresponds to narrow Raman bands, the apatite phase is generally well defined.
v. Group D_5 can be drawn on both sides of the dashed black diagonal line. This dashed black diagonal line underlines a widening of the band at ~820 cm^{-1} (which correlates with an increase in its area) trends that can be considered as a crystallinity effect. Since crystal growth at low temperatures or during a very short firing cycle is not possible, more disordered phases are formed under these conditions. This group includes samples of painted enamels on metal (#25–29,32–33: F1467; #36: F1698C; #39,44: R957; #48: R975) and on Chinese porcelain (#52: TH457), as well as underglaze decoration of European soft-paste porcelains (#6: MNC13369; #14: MNC26296; #15: MNC6638). Samples #34 and #35, which represent blue painted enamels on metal, respectively on objects F1467 and F1698C, are found marginal to these four groups.

The objective is to link these Raman signatures identified on ancient objects to the different structures identified in the literature. Remember that the phases present in the enamels are inserted in a matrix which can lead to structural distortions different from those synthesized in the isolated state (stress-induced structural distortion).

3.3 | PCA conducted on a selected spectral window: comments for reference spectra of the literature

As we are trying here to differentiate several profiles of the main peak located at ~820 cm^{-1} with potentially a shoulder at ~775 cm^{-1}, we focus the PCA on a reduced range of the Raman spectra between 720 and 880 cm^{-1}. This range excludes most of the contribution of the silicate matrix. A PCA on the whole spectra, that is, between 100 and 1200 cm^{-1} (see Supporting Information), is of no interest here because, as we have demonstrated in the companion paper[10] on yellow pigments, the definition of clusters would then rely more on the difference between the silicate matrices and of the relative intensity of the opacifier versus the glassy matrix. In particular, for the set of spectra considered here (see Figure 3), the Raman signatures of the deformation modes and of the stretching modes of SiO_4 tetrahedron, respectively, around 500 and 1100 cm^{-1}, are indeed much more dominant than the characteristic peak of As-O type structures, which is not particularly associated with other significant bands.

We will consider that the spectra do not correspond to a particular polarisation but the spectrum of an almost randomly oriented set of grains.

As visual observation of the spectra in Figure 1 already shows, the Raman signatures in the range between 720 and 880 cm^{-1} of the four olivine types from the literature references stand out clearly from the signatures of the other references and enamel samples with the presence of a pronounced doublet of peaks for fayalite, forsterite and Ni-olivine and with peak positions at much higher values for Co-olivine (shoulder at ~816 cm^{-1} and main peak at ~858 cm^{-1}).

This difference in profiles and/or peak positions is well reflected in the PCA conducted on all enamel samples and references from the literature (Figure S1). Comparison of the two main PCA components clearly differentiates the olivine group from that of arsenic-based phases, with much lower values on the first component for references of the olivine family (Figure S1A). However, according to the spectrum of PC1 in the loading plots (Figure S1C), the negative values for PC1 correspond to the Raman signatures with the highest intensities in the ~820- to ~860-cm^{-1} range. This matches well with the position of the olivine peaks being at higher values, as mentioned earlier. A few European porcelain

glazes are distributed close to olivine references (Figure S1B). These are opacified with tin, revealing a peak at ~775 cm^{-1} more pronounced than just a shoulder, creating a double-peak profile similar to that of three of the four olivine samples. However, as the positions of the latter are at much lower values, we reject the hypothesis that the signatures recorded in these enamels correspond to those of olivine-type phases.

In the following, we will therefore use only the arsenic-based references for comparison. Figure 6A,B compare thus the two main PCA components of spectra of the (Figure 6A) 23 As-based references from literature[18,25–28] (Table S2) and (Figure 6B) 52 measurements on enamelled artefacts (Table S1), once SNV normalization was performed on the defined interval. Figure 6C shows the loading plots of PC1 and PC2 resulting from this PCA. The difference between its two subfigures is that in the first (a), only the reference samples are shown. We observe two neighbouring clusters in Figure 6A, the first showing negative values on PC1 and the second positive ones. The first cluster is constituted by 10 of the 12 lacunar apatites ($Na_{1-x}K_xPb_4(AsO_4)_3$) that the references count.[18] The hydrated wendwilsonite reference [$Ca_2Mg(AsO_4)\cdot 2H_2O$] observed in an English delftware glaze (c. 1770) could be due to some surface corrosion,[28] as well as the hedyphane reference [$Pb_3Ca_2(AsO_4)_3Cl$] from Frost et al.,[25] but which was also observed in glazes from English delftwares,[28] are also found in this cluster. Two $Na_{0.5}K_{0.5}Pb_4(AsO_4)_3$ references are more isolated from this main cluster. Their spectra differ from those of similar phases by the position of their stronger peak at 812–813 cm^{-1} versus 816–818 cm^{-1}.[18] The second is represented notably by the references of As-doped lead hydroxyl apatite[27] and mimetite,[25] phases that can be considered as formed by corrosion of apatite. As can be seen from the blue spectrum of PC1 in the loading plots shown in Figure 6C, samples with negative values for this component are those for which the centre of gravity of the main peak of the As-O bond is located beyond ~820 cm^{-1}. As the value of PC1 becomes more negative, the position of the centre of gravity increases, with a maximum at around 833 cm^{-1}. In addition, looking at the profiles of the corresponding spectra, the factor that separates these two trends is the shoulder at 775 cm^{-1}. It is less marked, or even absent, in references from the second cluster.

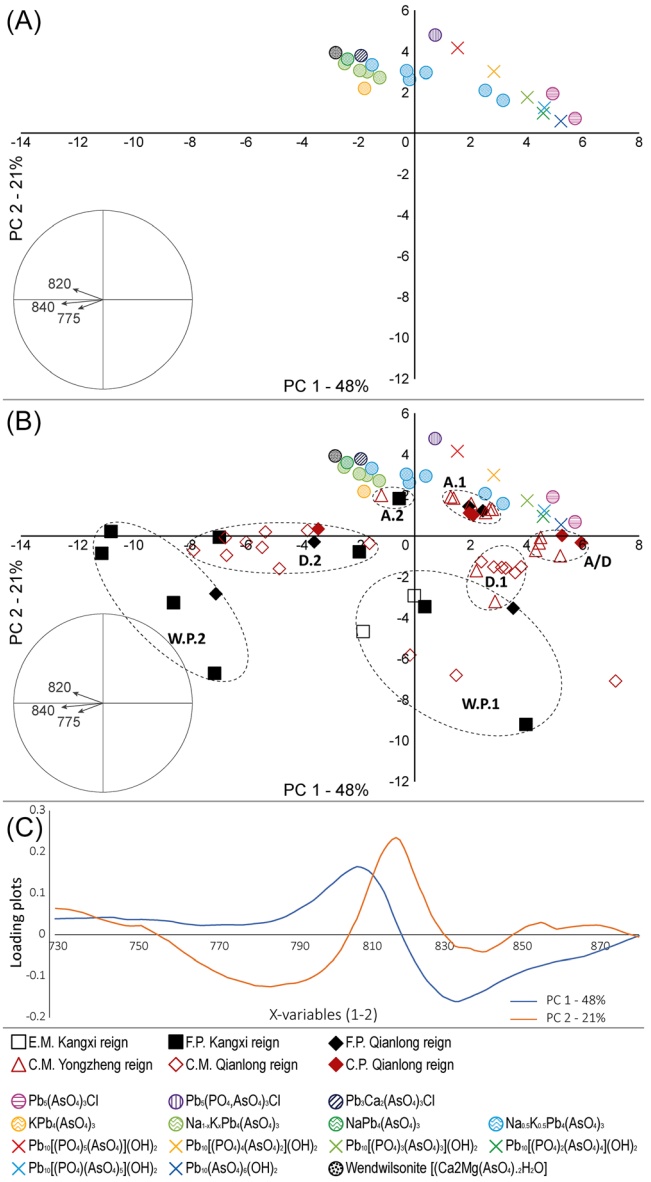

FIGURE 6 Diagrams from PCA analysis with the first and second components calculated on the spectra within the 730- to 880-cm^{-1} interval from the corpus of the studied objects plus all the phases from the literature featuring the main As-O peak around 820 cm^{-1}: (A) references[18,25–28] only; (B) references[18,25–28] and studied objects[5,17,21–24]; (C) loading plots showing the projection of PC1 and PC2 on the initial variable space. The inset circles represent the contributions of three of the wavenumbers used in the PCA calculation. In the legend, M: metal ware; P: porcelain; E: European; F: French and C: Chinese.

3.4 | PCA conducted on a selected spectral window: comments for measured spectra

By considering the data of enamelled samples within the binary diagram of the PCA (Figure 6B), we can define seven clusters that can be related to the three main Raman spectral profiles of the As-O bond peak shown in Figure 4.

Two clusters—A.1 (Apatite 1) and A.2 (Apatite 1)—clearly correspond to Raman signatures similar to that of apatite (Figure 4C). Cluster A.1 represents the samples with the positive values on the two principal components

and all Raman signatures contain the As-O peak located between 812 and 816 cm^{-1} associated with a shoulder between 766 and 773 cm^{-1}. This group is very diverse in terms of types of objects since it represents two French porcelains (#14 MNC26296 and #16 MNC25330), one Chinese porcelain (#23–24 F1429C) and one Chinese metallic plate (#38–40,42,45–46 R957). This cluster appears to be associated with the two marginal $Na_{0.5}K_{0.5}Pb_4(AsO_4)_3$ references that were fired to the highest temperatures (300°C and 350°C) of Manoun et al.'s study.[18] A shift to lower wavenumbers is observed between the spectra of this apatite cluster A.1 and those of the apatite cluster A.2.

Cluster A.2 consists of two samples with a French porcelain glaze (#6 MNC13369) and an overglaze enamel of the Chinese metal plate R957 (#44). What differentiates the Raman signatures of these two samples from those of group A.1 is indeed the position of the two peaks around 775 and 820 cm^{-1} at higher values; in this case 776 and 819 cm^{-1} for #6 and 768 and 819 cm^{-1} for #44. The position of the two samples constituting A.2 is relatively close to the main group of apatite references. We can expect that these clusters correspond to two different distortions of apatite structure.

Note that the Raman signatures of the enamel samples from these two groups do not attest to the presence of cassiterite (SnO_2), a second type of opacifier, largely used in French productions.[23,43,49,50]

The third group of samples that present a signature similar to those of some references is the group called A/D (Apatite/Disordered) in Figure 6B. We name it that way because the profile of the As-O stretching vibration band is an intermediate between (or superimposition of) the apatite type peak and the disordered peak, since it presents a not quite pronounced shoulder. The position of the main peak for the A/D samples is between 810 and 812 cm^{-1}. The two Chinese objects are within this group, a metallic bottle (#17–20 F1341C) and a porcelain teapot (#21–22 F1429C). For the Raman signature of references phases close to the signatures of Group A/D enamels, the shoulder around 775 cm^{-1} is less noticeable.

The four remaining sample groups do not correlate with any reference groups.

These clusters include W.P.1 (Weak Peak 1) which contains seven samples which, among those with positive values on the first component, have the most negative ones on the second. These samples exhibit a weak As-O peak around 820 cm^{-1} and a rather strong peak around 775 cm^{-1}, such as those shown in Figure 4B. Moreover, the ratios of the areas of the 820/775 cm^{-1} peaks calculated for the samples of this cluster are the lowest of the whole corpus. Note also that the position of the stronger peak varies between 819 and 823 cm^{-1} among these samples. The narrow peak at ~775 cm^{-1} seems to be more a result of the presence of cassiterite, which is detected in all the samples of this cluster and is characterized by a 635–775 cm^{-1} doublet,[43] except for #9, thanks to its main peak located around 635 cm^{-1}. The fact that the Raman profile of the two peaks considered for treatment depends on two phases (i.e., cassiterite and arsenate(s)) and not only one as in most other clusters, explains why the distribution of the samples in W.P.1 is relatively diverse. Regarding the type of samples in this group, we find the two painted glazes on European watches (#1 OA10079 blue and #2 OA8435 blue), three glazes of French porcelains (#9 MNC4006 blue, #12 MNC8800 blue, #13 MNC8102 blue), and two glazes of Chinese object F1467C (#25 green and #30 yellow).

The other group in which the distribution of samples is also disparate, named W.P.2 (Weak Peak 2), concerns the second cluster that represents enamels whose Raman signature also contains the weak As-O peak. It concerns five samples that have among the lowest values on the first component (Figure 6B). Of these five samples, four have a weak As-O peak; only #11 MNC4027 has an apatite-like peak as shown in Figure 4C. It is likely that the low intensity of the Raman signals leads to the separation of this type of spectra. One of the main differences that these samples have from those in the W.P.1 group is the position of the "820 cm^{-1}" peak located at higher values, between 829 and 836 cm^{-1}. Only blue enamels #3–4 of MNC17063 contains cassiterite, which explains their relatively strong peak at ~775 cm^{-1}. Another particularity of these two enamels is the presence of a peak at 867 cm^{-1} characteristic of chromate.[13] We will discuss this second characteristic later. The three other blue enamels #5 MNC18433, #10 MNC18432 and #11 MNC4027 do not contain cassiterite. The shoulder they show at 775 cm^{-1} should be more related to an apatite-type phase. In this group W.P.2 appear only French soft-paste porcelains.

The two last groups concern Raman spectra featuring the broad As-O peaks (Figure 4D) represented by clusters D.1 (Disordered 1) and D.2 (Disordered 2) in Figure 6B. The Raman signature of the samples from these two groups is indeed illustrated by a broad band around 820 cm^{-1} and the absence of the shoulder around 775 cm^{-1}. What differentiates the two groups is the position of this main band, since it varies between 809 and 812 cm^{-1} with the samples of D.1 and between 816 and 830 cm^{-1} with the samples of D.2. It is interesting to observe that the samples of group D.1 are all

painted enamels on Chinese metal objects produced in Ganzhou (#35 F1698C; #41,43 R957 and #47–51 R975), while those of group D.2 concern two French porcelains (#7–8 MNC13371 and #15 MNC6638), two Chinese metal ware from different workshops (#26–29,31–34 F1467C and #36 F1698C) and one Chinese porcelain (#52 TH457). Note that the Raman signatures of the samples in these two clusters do not attest to the presence of cassiterite. This splitting probably reflects different (or variations in) production processes.

Since the spectra of all references were characterized by this "820 cm^{-1}" peak with a more or less pronounced shoulder around 775 cm^{-1}, this explains the reason why neither the groups W.P. nor the groups D are found associated with one or more of these references.

We can see that the resulting PCA classification shown in Figure 6 depends on the first two PCs, whose cumulative variance is 69%, which may seem relatively low. However, as the diagrams in Figures S2 and S3 show, comparing respectively the distribution of samples according to PC2 (21%) versus PC3 (13.5%) and PC1 (48%) versus PC4 (8.8%), we find a similar classification of groups, but which seems less obvious. We note, however, that it is really the first PC that is the most discriminating, separating the samples according to the position of the main peak at around 820 cm^{-1}. PC3 allows us to identify the different signatures of the shoulder at ~775 cm^{-1} (Figure S2). Indeed, the samples distributed in the positive values of PC3 are those showing a pronounced shoulder, namely, among others, apatite references as well as enamels from groups A.1 and A.2 and those from groups W.P.1 and W.P.2. The rather low concentration of variance in the first principal components reflects the structure of the data. They do not allow a strong discrimination between samples. A significant proportion of the variance does not structure the data, indicating either that not enough samples have been studied (statistically representative for each group), or that the information potential is too low.

In sum, the constitution of these seven clusters thus follows the categorization of the profiles of the As-O bond peak as presented in Figure 4. However, each of these three categories of peaks (three different structure/unit-cell?) separates into two subgroups (vacancy non-stoichiometry?) according to the position of the "820 cm^{-1}" peak, as illustrated by the loading plots (Figure 6C) and the formation of the two large anti-correlated clusters in Figure S2. X-ray microdiffraction study and structure refinement are required to go further in the understanding of the categorization. The samples to the right of the y-axis, from clusters A.2, D.2 and W.P.2, are those with the "820 cm^{-1}" peak centred at larger wavenumbers.

3.5 | PCA conducted from spectroscopical data extracted by spectral decomposition

We now performed PCA on the data extracted from the spectral decomposition. The variables considered are the centre of gravity, the width at half height and the area of the characteristic peaks located around 775 and 820 cm^{-1}. Figure 7 shows the distribution of the enamel samples and of the reference As-based phases extracted from literature, of which some are presented in Figure 2 (lead arsenates), according to the first and second component calculated for the PCA. We find that this comparison allows us to separate the corpus into two main groups (Figure 7). The references from the literature are globally grouped together in a third, partially separate group.

The group of samples with positive values for the first component and negative values for the second component has 24 individuals. The characteristic of the samples in this group is that they have the largest A820/A775 ratios. We thus find in this group all the samples whose peak profile is similar to that shown in Figure 4C, namely, groups A.1 and A.2 presented in the previous

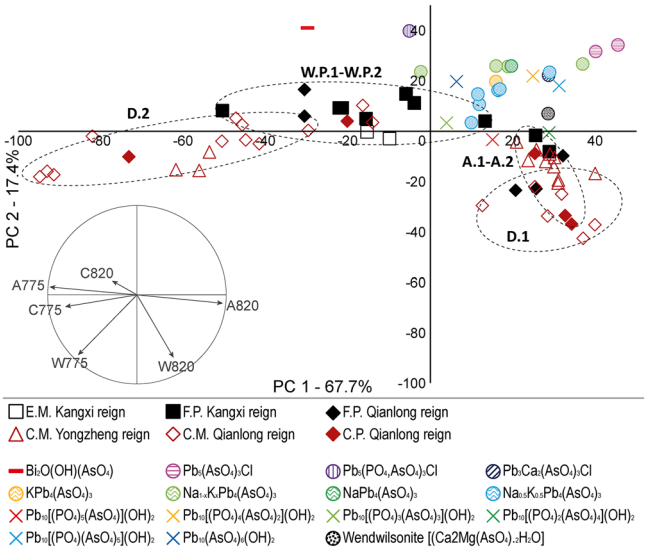

FIGURE 7 PCA diagram of the first and second components calculated with the parameters extracted from the spectral decompositions on the corpus of the studied objects (Table S1) plus all the phases from the literature (Table S2) featuring the main As-O peak around 820 cm^{-1} (variables are the centre of gravity, the width and the area of the peaks at ~775 and ~820 cm^{-1}; centring option: yes; scaling option: no; number of PC max: 20). The inset circle in the diagram represents the contributions of the variables in the principal components plane under consideration. In the legend, M: metal ware; P: porcelain; E: European; F: French and C: Chinese.

section. Seven of the eight samples of group D.1 also belong to this group, as do only three samples of group D.2 and two of group A/D. In this group, the lower the values of the second principal component, the higher the width of the "820 cm^{-1}" peak. Therefore, we find all the samples of the D.1 group among the subcluster of samples with second principal component values lower than −20, while 10 of the 13 samples of the two apatite groups (A.1 and A.2) are found in the subcluster with values higher than −20.

The second group of samples gathers the Raman signatures that show the ∼775 cm^{-1} peak at the highest wavenumbers. In this group, the lower is the value of the first principal component, the higher the peak wavenumber. Among the samples with a value of the second component higher than −30, we find mainly the weak As-O peaks with three samples from the group W.P.2 and six of the seven samples from the group W.P.1, plus one sample from A/D and one from D.2. The samples with a value of the second component lower than −40 represent mostly the group D.2 since they concern eight of the 13 samples of this subgroup; the other five belonging to the D.1 (1), W.P.1 (1) and A/D (3) groups.

Concerning the group of the literature references phases for which the values in the two main components are positive, it differs mainly from the two sample groups by the width of the "820 cm^{-1}" peak, which is the smallest for the references. The more pronounced narrowness of the Raman peaks of references can be explained by the fact that the phases are synthesized "pure" and specifically for structural studies with thermal treatments developing the crystallinity, while the broader peaks of the As-O bonds observed in the enamel matrix are those of phase issue of natural raw materials and with a lower crystallinity. It should be noted that the wendwilsonite reference, the only nonsynthesized reference observed in an English Delftware glaze, is located on the binary diagram relatively close to the cluster of samples from A.1 and A.2 groups.

The PCA performed on the variables obtained from the spectral decomposition proposes a different classification of the samples than the one obtained from the spectra, but which still follows a similar logic. Indeed, in the group defined mainly by the position of the 775 cm^{-1} peak at higher wavenumbers, the samples from groups W.P.1 and W.P.2 are present, for which the presence of this peak is justified mainly by the presence of cassiterite. Also present are the samples of group D.2, namely, those having the disordered apatite band with the position of the main band at ∼820 cm^{-1} among the highest values (816–830 cm^{-1}), entailing de facto the position of its first band at higher wavenumbers mainly between 790 and 815 cm^{-1}, which we consider here as the "775 cm^{-1}" band. The second cluster of samples has the highest A820/A775 ratios, hence the fact that we find here members of groups A.1 and A.2 as well as most of the samples of group D.1. On the other hand, because of their narrower As-O band bandwidth, it is not possible, in this case, to associate references phases with the Raman signatures recorded on the enamels.

4 | DISCUSSION ON THE EFFECTIVENESS OF THE PROCEDURES

4.1 | Comparison between the spectroscopic (Figure 5) and PCA/hierarchical clustering approach (Figure 8)

The PCA performed both directly from the spectra, and by using the variables obtained after performing spectral deconvolution, confirm the classification achieved on the basis of the main As-O band profiles by visual observation of the Raman parameters used to build Figure 5 (five groups identified). The PCA performed on the spectra brings however additional components to this classification, because it takes into account not only the shape of the "820 cm^{-1}" and "775 cm^{-1}" bands, but also their position and their ratio of areas. It thus allows a classification of the spectra according to seven groups (plus two isolated spectra: #11 and #37), which we can present schematically thanks to the dendrogram of Figure 8. This agreement between spectroscopic assignments summarized Figure 5 and multivariate analysis can be highlighted as follows. In Figure 8, all but #25 of the samples in group W.P.1, belong to group B_5 of the diagram in Figure 5. All samples in group A/D are also in group C_5 of Figure 5, while 14 of the 18 samples in the set of groups A.1 and D.1 fall into groups C_5 and C'_5. The two samples from A.2 fall into group D_5, as do the samples from group D.2 except #31, and the samples from group W.P.2 fall into group A_5 in Figure 5.

4.2 | The "weak intensity peak" groups

Two groups are identified in this category presenting a weak As-O peak with the so-called W.P.1 (B_5) and W.P.2 (A_5). In fact, we can consider that there are rather three because two spectra profiles appear in the W.P.2 group. All the enamels of the European objects of group W.P.1 are blue and are opacified with

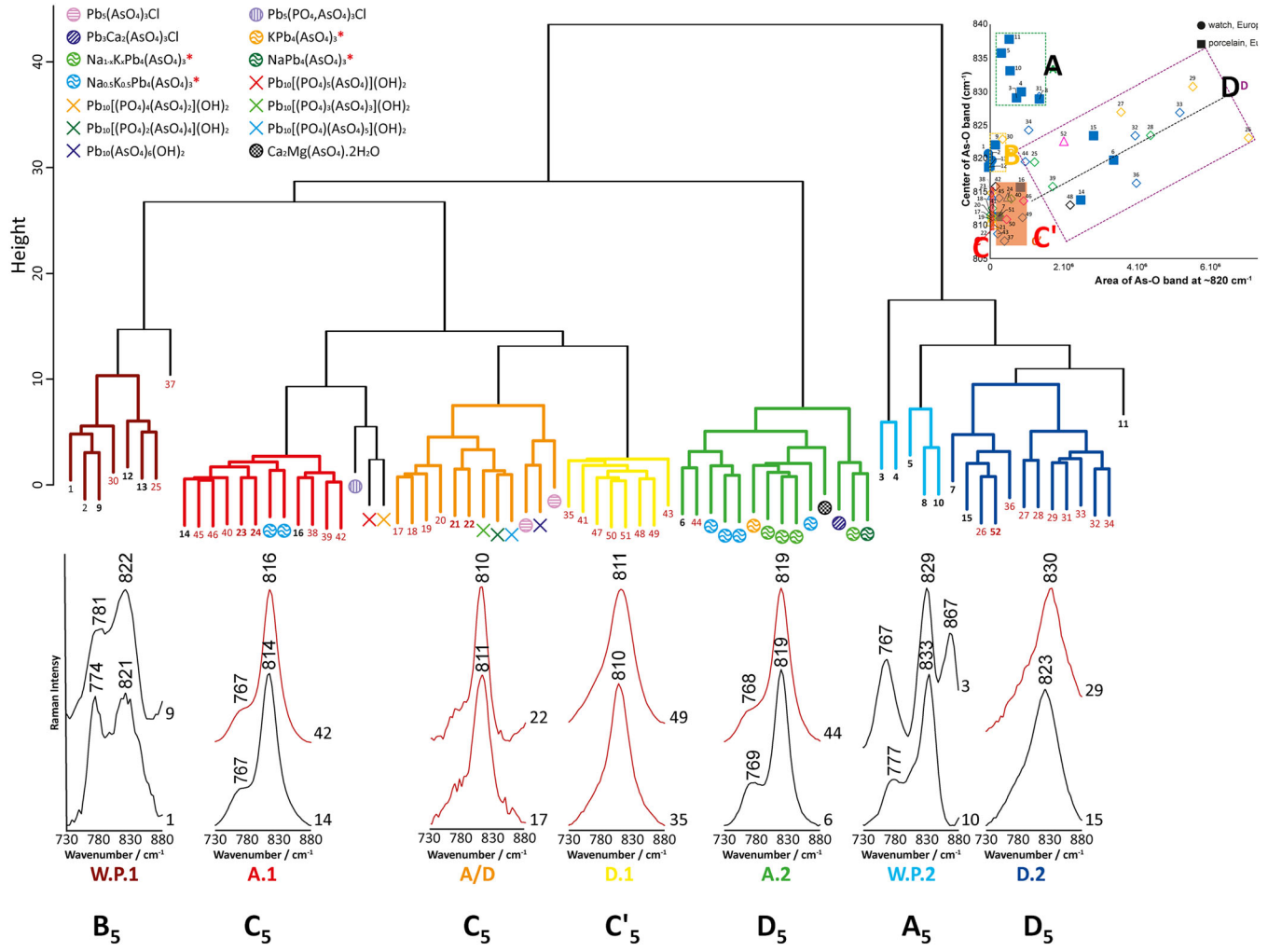

FIGURE 8 Hierarchical clustering using the Euclidian distance and the Ward's aggregation rule on the spectra, within the 730- to 880-cm^{-1} interval, of the studied objects and of the reference phases from the literature (scaling option: no; choice of cluster number: 4). Codes of the samples (id. Numbers) are as follow: black for European objects, red for Chinese ones and bold for porcelains. Red asterisk represents references from Manoun et al.[18] Typical spectral profiles for each group are shown below the dendrogram (see Table S1 for the correspondence with the artefact number). The corresponding groups identified in Figure 5 (given again in the form of a small insert) are also given (X5). The spectral characteristics of the highlighted groups and the samples that comprise them are summarised in Table 1.

cassiterite that pollutes the Raman spectrum in the range where bands characteristic of lead arsenate are present. In the spectral window considered, their Raman spectra, with a narrow peak around 775 cm^{-1}, correspond to the second main band of cassiterite. The presence of the As-O band around 820 cm^{-1} would result more from phase(s) related to arsenic impurities present in the blue cobalt pigment imported from Europe.[13,22] This trace amount of arsenic in the glaze would justify why we record a weak peak of the As-O bond in Raman spectroscopy. Contrary to the European samples, where cassiterite is a deliberate opacifier, the presence of this phase in the two Chinese glazes (including exceptional F1467C ewer), one yellow and the other green, is more likely the result of the use of the complex Naples yellow pigment presented in the companion paper[10] in this same volume on yellow. Tin provided by the addition of Naples yellow precipitates as cassiterite. The presence of the As-O peak in these two enamels illustrates the use of arsenic as an opacifier, as evidenced by its presence in the other enamels of this same object for which no cassiterite is detected.

As mentioned earlier, the samples of group W.P.2 (A_5) seem to represent two categories of phases. Indeed, we have samples #3 and #4 which show both cassiterite, As-O bond and probably chromate bands (Figure 8: spectrum 3, chromate also exhibit strong Raman peak around 830–850 cm^{-1}),[13,43,51] and the other three samples #5, #8

TABLE 1 Summary of the different groups of Raman signature of the band associated with the main As-O stretching vibration around 820 cm^{-1} shown in Figure 8 (mp: main peak; sh: shoulder).

Group	Characteristic bands	Productions
W.P.1	Sn-O: 774–784 cm^{-1} As-O: mp at 819–823 cm^{-1}	European metallic watch French soft-paste porcelain Chinese (Imperial Palace workshop) metal ware
W.P.2	Sn-O: 767–770 cm^{-1} (#3 and #4) As-O: mp at 829–830 cm^{-1} (#3 and #4) Chromate: ∼867 cm^{-1} (#3 and #4) As-O: sh at 774–785 cm^{-1} (#5, #8 and #10) As-O: mp at 829–836 cm^{-1} (#5, #8 and #10)	French soft-paste porcelain
A.1	As-O: sh at 766–773 cm^{-1} As-O: mp at 812–816 cm^{-1}	French soft-paste porcelain Chinese (Imperial factory of Jingdezhen) hard-paste porcelain Chinese (Private workshop at Guangzhou) metal ware
A.2	As-O: sh at 768–776 cm^{-1} As-O: mp at ∼819 cm^{-1}	French soft-paste porcelain Chinese (Private workshop at Guangzhou) metal ware
A/D	As-O: mp at 810–812 cm^{-1}	Chinese (Imperial factory of Jingdezhen) metal ware and porcelain
D.1	As-O: mp at 809–812 cm^{-1}	Chinese (Private workshop at Guangzhou) metal ware
D.2	As-O: mp at 816–830 cm^{-1}	French porcelain Chinese (Imperial Palace workshop) metal ware Chinese (Private workshop at Guangzhou) metal ware Chinese (unknown workshop) hard-paste porcelain

and #10 for which the peak profile is more apatite-like. Although two subgroups can be distinguished in this group, it represents only soft-paste French porcelain. In the first subgroup, represented by samples #3 and #4, both from MNC17063, we are faced with the use of a cassiterite opacified glaze and whose blue painted decoration required the use of an arsenic-rich smalt[13] associated with chromium traces. The Raman spectra profile of the As-O stretching mode of the three other samples, representing three other French porcelains (MNC18433, MNC13371 and MNC18432), is more similar to that of apatite (Figure 8: spectrum 10). Moreover, for sample #8, the Raman spectrum shows evidence of a very strong As-O stretching mode (Figure 4C), not a weak one, which likely reflects the analysis of a large lead arsenate globule.[22] The blue pigment used for these three samples is therefore also of the European As-rich cobalt type, but whose preparation and/or raw materials employed were different from those of the pigment used for the decoration of porcelain MNC17063, as well as for that of the W.P.1 group objects for which the values recorded for the As-O band position are lower.

4.3 | The "apatite" groups

We count among the apatite signature the two groups A.1 (C_5) and A.2 (D_5) of course, as well as the group A/D (C_5) because, as shown in the dendrogram in Figure 8, it includes notably the two references of mimetite.

Group A.1 differs from group A.2 due to the slight shift to lower values of the position of the "820 cm^{-1}" peak and the "775" shoulder (see spectra in Figure 8).

For the three French porcelains belonging to the groups of "apatites" from the structural description point of view—MNC13369, MNC26296 and MNC25330—dated to the early-mid 18th century, the observation of this apatite-like phase with notably this strong band of As-O stretching mode probably attests to the use of an arsenic-rich ore for the production of the underglaze blue decoration.[22]

Concerning the enamels painted on the Chinese metal ware R957, the presence of this peak shows the use of arsenic as an opacifier. Indeed, the enamels in question are here of several colours and therefore not exclusively blue, which does not allow the hypothesis of an exclusive contribution of arsenic by the use of a European cobalt pigment. However, we note that the blue enamel #44 belongs to group A.2, while all the other enamels of this object are in group A.1. Could the presence of this blue enamel in group A.2 with a shift in peak positions compared to group A.1 be explained by the influence of both the arsenic-based opacifier and the arsenic-rich cobalt in the Raman signature? Or is it that the fact of preparing enamels of different colours

and therefore different raw material provenance or firing temperature leads to different reactions during firing that would cause this shift? These questions are still open, and we will find that we will also ask them for the next sample. Surface corrosion (hydroxylation) is also possible.

The Chinese porcelain F1429C produced in Jingdezhen has indeed its two blue enamels present in group A.1, while its two yellow enamels are in group A/D. In this case, the presence of the arsenic-based apatite phase is also explained by its use as an opacifier.

Four other glazes (#17–20) painted on the metallic bottle F1341C assigned to be produced in Jingdezhen are present in group A/D. Among the apatite groups, A/D has the lowest peak position of the As-O bond, between 806 and 814 cm^{-1}.

A correlation seems to emerge between these three subgroups of apatites and the types/places of production of the objects concerned. Indeed, groups A.1 and A.2 include three samples of French porcelain as well as enamels painted on metal from a workshop in Guangzhou, plus two enamels painted on porcelain from Jingdezhen, while group A/D consists only of enamels assigned to Jingdezhen kilns.

4.4 | The "disordered" groups

Let us recall that the broadening of the band at ~820 cm^{-1} is consistent with the formation of a more disordered phase, or with a smaller size of the crystals (typically < 20–50 nm).[52] The two groups reflecting these disordered phases are D.1 (C'_5) and D.2 (D_5), which differ, in their Raman signature, from the position of the centre (see spectra in Figure 8) and the total area of the main band at ~820 cm^{-1} (see group C-C′ for D.1 and group D for D.2 in Figure 5). These differences probably illustrate new-formed phases under different firing and/or matrix conditions, and therefore differences in the production techniques used.

This hypothesis seems to be confirmed as we note that only painted enamels on metal objects produced in Guangzhou are present in group D.1, while group D.2 concerns only enamels from object F1467C produced in the palace in Beijing, as well as a glaze from a French porcelain (#15 MNC6638) and a painted enamel from a Chinese porcelain (#52 TH457). In the case of the Chinese enamels, given that they concern several colours, the presence of this arsenic-based phase refers to the use of this element as an opacifier. As for its presence in the blue decoration of French porcelain, it is probably the result of the use of smalt.

5 | CONCLUSION: COMPARISON OF THE APPROACHES AND IMPLICATION ON THE ENAMELLING TECHNIQUES

In sum, the combination of classifications derived from comparison of the spectra characteristics (Figure 5), those obtained from multivariate analysis of the spectra, or parameters extracted from spectral decomposition (Figure 8) lead to similar conclusions. The relatively high number of cluster identified by the different approach show the complexity of the identification of phases by Raman scattering only. The shape, position and area of the band associated with the main As-O stretching vibration around 820 cm^{-1} vary according to several criteria related to production techniques specific to certain workshops. This should correspond to different phase distortion (variable symmetry, amount of oxygen vacancies, etc.) or association of phases determined by the firing cycle. For example, in the cassiterite-opacified blue glazes of French porcelains, the peak has a low intensity because it probably corresponds to traces of arsenic from a cobalt pigment powdered and then directly painted on the ceramic surface.[22] Associated with this weak peak around 820 cm^{-1} is an equally or more intense peak at ~775 cm^{-1} characteristic of cassiterite. This is likely a similar pigment used in the blue enamels of the two European watches dated to the late 17th-early 18th century.

From the beginning-middle of the 18th century, the production techniques for the glaze of French porcelain changed (soft- to hard-paste porcelain). These are no longer opacified with tin and the blue colour originates from the use of arsenic-rich ore.[22] The use of this pigment leads to the formation of large globules of lead arsenate in the lead-rich silicate matrix, as shown by electron microscopy[53] and their analysis by Raman microspectroscopy records a very strong As-O stretching mode band.

In Chinese enamels, this band around 820 cm^{-1} is always recorded with a high intensity. A good crystallization of the phase leads to a band characteristic/similar to that of apatites. In such a case, it is to be presumed that the craftsmen mastered the firing process, which seems to be the case of the porcelain produced at imperial workshops of Jingdezhen, because all the bands recorded in the glazes of the objects produced there have this characteristic shape. The enamels of an object from Guangzhou also show this phase assimilated to apatite, while the enamels of the two other metalwares from Guangzhou have the broad band at ~820 cm^{-1}, assimilated to a disordered phase related to a noncomplete crystallization. The same is true for the enamels of the enamelled metalware F1467C assigned to be produced in the workshop of

the imperial palace of Beijing, but whose position and intensity of the Raman signatures of the disordered phase are different from those recorded in the Guangzhou enamels. Usually enamels on metal are fired at lower temperature than overglaze on porcelain that fit with a lower crystallinity.

While in part I of this work concerning Naples yellow/pyrochlore pigments the contribution of multivariate analysis procedures demonstrated their effectiveness,[10] in the case of lead arsenates, the effectiveness appears to be much lower than that resulting from a usual spectroscopic analysis. It is advisable to try to identify the points which limit the effectiveness. In the case of pyrochlore and associated phases, not only spectra of perfectly identified structural phases were available in the literature, but in addition the characteristic spectrum of the different variants is distinguished by the presence of additional peaks and/or significant displacements of the peaks wavenumbers. On the contrary, in the case of lead arsenates, both there is a lack of reference spectra and the variations mainly concern a small spectral window, with the number of peaks being reduced to two and variations mainly affecting their widths. As expected, a large number of characteristic peaks/informative parameters favours the efficiency of a multivariate analysis.

ORCID

Jacques Burlot https://orcid.org/0000-0002-6451-1788
Divine Vangu https://orcid.org/0009-0004-6474-0304
Ludovic Bellot-Gurlet https://orcid.org/0000-0002-7995-6261
Philippe Colomban https://orcid.org/0000-0001-6099-5423

REFERENCES

[1] P. Colomban, *J Raman Spectrosc* **2012**, *43*, 1529.
[2] P. Colomban, in *Modern Methods for Analysing Archaeological and Historical Glass*, 1st ed. (Ed: K. Janssens), John Wiley and Sons Ltd, London **2012**, 275.
[3] P. Colomban, *J Raman Spectrosc* **2018**, *49*, 921.
[4] H. G. M. Edwards, P. Vandenabeele, P. Colomban, *Raman Spectroscopy in Cultural Heritage Preservation*, Springer, Cham, Switzerland **2022**.
[5] P. Colomban, B. Kırmızı, B. Zhao, J.-B. Clais, Y. Yang, V. Droguet, *Heritage* **2020**, *3*, 915.
[6] M. C. Caggiani, P. Colomban, C. Valotteau, A. Mangone, P. Cambon, *Anal Methods* **2013**, *5*, 4345.
[7] P. Colomban, A. Tournié, *J Cult Herit* **2007**, *8*, 242.
[8] C. Ricci, C. Miliani, F. Rosi, B. G. Brunetti, A. Sgamellotti, *J Non Cryst Solids* **2007**, *7*(353), 1054.
[9] J. Van Pevenage, M. Baeck, E. Verhaeven, L. Vincze, L. Moens, P. Vandenabeele, *J Cult Herit* **2020**, *41*, 27.
[10] P. Ricciardi, P. Colomban, A. Tournié, V. Milande, *J Raman Spectrosc* **2009**, *40*, 604.
[11] P. Colomban, B. Kırmızı, *J Raman Spectrosc* **2020**, *51*, 133.
[12] S. A. Kissin, *Geosci Canada* **1992**, *19*, 113.
[13] P. Colomban, B. Kırmızı, G. Simsek Franci, *Minerals* **2021**, *11*, 633.
[14] P. Colomban, G. Simsek Franci, M. Gironda, P. d'Abrigeon, A.-C. Schumacher, *Heritage* **2022**, *5*, 1752.
[15] P. Colomban, M. Gironda, G. Simsek Franci, P. d'Abrigeon, *Materials* **2022**, *15*, 5747.
[16] P. Colomban, *Materials* **2022**, *15*, 3158.
[17] P. Colomban, B. Kırmızı, B. Zhao, J.-B. Clais, Y. Yang, V. Droguet, *Coatings* **2020**, *10*, 471.
[18] B. Manoun, M. Azdouz, M. Azrour, R. Essehli, S. Benmokhtar, L. El Ammari, A. Ezzahi, A. Ider, P. Lazor, *J Mol Struct* **2011**, *986*, 1.
[19] P. Colomban, G. Simsek Franci, J. Burlot, X. Gallet, B. Zhao, J.-B. Clais, *Ceramics* **2023**, *6*, 447.
[20] P. Colomban, A.-T. Ngo, N. Fournery, *Heritage* **2022**, *5*, 233.
[21] P. Colomban, B. Kırmızı, C. Gougeon, M. Gironda, C. Cardinal, *J Cult Herit* **2020**, *44*, 1.
[22] P. Colomban, T.-A. Lu, V. Milande, *Ceram Int* **2018**, *44*, 9018.
[23] P. Colomban, M. Gironda, H. G. M. Edwards, V. Mesqui, *J Raman Spectrosc* **2021**, *52*, 2246.
[24] P. Colomban, M. Gironda, D. Vangu, B. Kırmızı, B. Zhao, V. Cochet, *Materials* **2021**, *14*, 7434.
[25] R. L. Frost, J. M. Bouzaid, S. Palmer, *Polyhedron* **2007**, *26*, 2964.
[26] R. L. Frost, J. Čejka, J. Sejkora, J. Plášil, B. J. Reddy, E. C. Keeffe, *Spectrochim Acta A Mol Biomol Spectrosc* **2011**, *78*, 494.
[27] A. Giera, M. Manecki, T. Bajda, J. Rakovan, M. Kwaśniak-Kominek, T. Marchlewski, *Spectrochim Acta A Mol Biomol Spectrosc* **2016**, *152*, 370.
[28] H. G. M. Edwards, W. H. Jay, *Spectrochim Acta A Mol Biomol Spectrosc* **2022**, *279*, 121458.
[29] WebPlotDigitizer, https://automeris.io/WebPlotDigitizer/ (accessed 22 November 2022).
[30] K. E. Kuebler, B. L. Jolliff, A. Wang, L. A. Haskin, *Geochim Cosmochim Acta* **2006**, *70*, 6201.
[31] C. C. Lin, *Phys Chem Min* **2001**, *28*, 249.
[32] P. Colomban, *J Cult Herit* **2008**, *9*, e55.
[33] Galaxy/ChemFlow 20.05, https://vm-chemflow-francegrille.eu/ (accessed 22 November 2022).
[34] J.-M. Roger, J.-C. Boulet, M. Zeaiter, D. N. Rutledge, in *Comprehensive Chemometrics: Chemical and Biochemical Data Analysis*, 2nd ed. (Eds: S. Brown, R. Tauler, B. Walczak) Vol. 3, Elsevier, Amsterdam **2020**, 1.
[35] R. J. Barnes, M. S. Dhanoa, S. J. Lister, *Appl Spectrosc* **1989**, *43*, 772.
[36] P. Colomban, A.-T. Ngo, H. G. M. Edwards, L. C. Prinsloo, L. V. Esterhuizen, *Ceram Int* **2022**, *48*, 1673.
[37] S. Pagès-Camagna, S. Colinart, C. Coupry, *J Raman Spectrosc* **1999**, *30*, 313.
[38] S. Pagès-Camagna, S. Colinart, *Arch Androl* **2003**, *45*, 637.
[39] D. Bersani, P. P. Lottici, A. Montenero, *J Raman Spectrosc* **1999**, *30*, 355.
[40] H. Berke, *Chem Soc Rev* **2006**, *36*, 15.
[41] R. J. H. Clark, M. L. Curri, C. Laganara, *Spectrochim Acta A Mol Biomol Spectrosc* **1997**, *53*, 597.
[42] P. Colomban, Routes du Lapis lazuli in Chine-Méditerranée, Routes et échanges de la céramique avant le XVIè siècle, Findakly, Taoci, vol 4, Suilly-la-Tour, **2005**, pp. 145–152.

[43] P. Colomban, G. Sagon, X. Faurel, *J Raman Spectrosc* **2001**, *32*, 351.
[44] M. Bouchard, A. Gambardella, *J Raman Spectrosc* **2010**, *41*, 1477.
[45] A. Pinto, P. Sciau, T. Zhu, B. Zhao, J. Groenen, *J Raman Spectrosc* **2019**, *50*, 711.
[46] T. Mouri, M. Enami, *J Mineral Petrol Sci* **2008**, *103*, 100.
[47] D. de Waal, *J Raman Spectrosc* **2007**, *38*, 956.
[48] M. L. Coutinho, J. P. Veiga, L. C. Alves, J. Mirão, L. Dias, A. M. Lima, V. S. Muralha, M. F. Macedo, *Appl Phys A: Mater Sci Process* **2016**, *122*, 696.
[49] P. Colomban, in *Conservation Science—Heritage Materials*, 2nd ed. (Eds: P. Garside, E. Richarson), The Royal Society of Chemistry, Cambridge **2019** 200.
[50] P. Colomban, in *Encyclopedia of Glass Science, Technology, History, and Culture*, (Ed: P. Richet), J. Wiley & Sons Inc., New York **2020**.
[51] P. Colomban, V. Milande, L. Le Bihan, *J Raman Spectrosc* **2004**, *35*, 527.
[52] G. Gouadec, P. Colomban, *Prog Cryst Growth Charact Mater* **2007**, *53*, 1.
[53] M. Maggetti, A. D'Albis, *Eur J Mineral* **2017**, *29*, 347.

SUPPORTING INFORMATION

Additional supporting information can be found online in the Supporting Information section at the end of this article.

How to cite this article: J. Burlot, D. Vangu, L. Bellot-Gurlet, P. Colomban, *J Raman Spectrosc* **2024**, *55*(2), 184. https://doi.org/10.1002/jrs.6612